

# Primary-Side-Converter-Assisted Soft-Switching Scheme for an AC/AC Converter in a Cycloconverter-Type High-Frequency-Link Inverter

Sudip K. Mazumder, *Senior Member, IEEE*, and Akshay K. Rathore, *Member, IEEE*

**Abstract**—Emerging trends of high-power-density power-electronics interfaces for renewable- and alternative-energy sources have led to the need for high-frequency-inverter designs without compromising energy-conversion efficiency. In that context, a zero-voltage-switching (ZVS)-based scheme is described in this letter, for a cycloconverter-type high-frequency-link inverter, which is applicable for renewable- and alternative-energy sources as well as other commercial applications. The proposed scheme achieves the primary-side-converter-assisted switching of the ac/ac converter switches under ZVS condition. The modes of operation of the ac/ac converter are explained to outline the behavioral response. The results on the efficacy of the ZVS-based inverter and its performance show satisfactory performances.

**Index Terms**—AC/AC converter, alternative, cycloconverter, energy sources, fuel cell, high frequency, high-frequency link, inverter, photovoltaic, renewable, zero voltage switching (ZVS).

## I. INTRODUCTION

HIGH EFFICIENCY, low cost, and high power density are important attributes of inverters for applications, including distributed-generation systems with renewable- and alternative-energy sources (e.g., photovoltaics, wind, and fuel cells), energy-storage systems, vehicle-to-grid applications, electric/hybrid-electric/fuel-cell vehicles, compact power conversion modules for naval, space, and aerospace applications, and battery-based uninterruptible power supplies. In such systems, galvanic isolation is often required for safety concerns and voltage and current scalabilities. In that regard, a high-frequency-transformer-based approach can be a preferable choice from the standpoint of weight, footprint, and cost reduction. Among the possible topologies, a high-frequency-link (HFL) pulsewidth-modulated (PWM) inverter can eliminate

the intermediate  $LC$  filter that is needed for a conventional high-frequency (HF) fixed-dc-link converter approach [1]–[3]. Furthermore, as compared to a resonant-link inverter, an HFL inverter yields lower switch stress, better total harmonic distortion (THD), and simpler all-device structure (i.e., no passive components within the power stages). Thus, the PWM HFL inverter approach is better suited from the viewpoints of cost, efficiency, and portability.

Two typical HFL inverter topologies have been proposed in the literature. One is a rectifier-type HFL (RHFL) inverter. It comprises a primary-side HF dc/ac converter feeding an HF transformer, which is followed by an ac/dc converter and a pulsating-dc/ac converter. Thus, the RHFL inverter topology possesses a structure similar to that of a conventional fixed-dc-link inverter except for the absence of the dc-link filter [4]–[9]. One of the features of the RHFL inverter topology is that the input signal to the output ac/ac stage is pulsating dc in nature (with encoded information of the primary-side HF dc/ac converter) that can be used to modulate the ac/ac stage with reduced switching loss [9].

The other class of topology is a cycloconverter-type HFL (CHFL) inverter, as illustrated in Fig. 1, which reduces the conversion complexity by directly placing an ac/ac converter to the secondary side of an HF transformer [10]–[23], which is fed by a primary-side HF dc/ac converter. In the CHFL topology, because the output stage is a single stage, the input to the ac/ac converter is an HF bipolar ac signal generated by the primary-side dc/ac converter. Therefore, switching the ac/ac converter using this primary-side converter information for switching loss reduction is a possibility. One such zero-voltage-switching (ZVS) mechanism, leading to reduced-loss switching with the assistance of a primary-side dc/ac converter, is outlined next in this letter which can be extended to a higher number of phases following the same principle.

## II. PRINCIPLE OF THE ZVS SCHEME

With reference to the CHFL inverter illustrated in Fig. 1, Figs. 2 and 3 show two switching schemes (for the ac/ac converter) that will be referred to as the “conventional scheme” and the new “ZVS scheme.” The operation of the HF full-bridge dc/ac converter (which remains the same for both the schemes), along with the operation of the conventional scheme, is described in detail in [18] and [22] and is not repeated in

Manuscript received July 14, 2010; revised October 24, 2010; accepted November 19, 2010. Date of publication December 10, 2010; date of current version August 12, 2011. The work of S. K. Mazumder was supported in part by the U.S. National Science Foundation CAREER Award 0725887, received in the year 2007.

S. K. Mazumder is with the Laboratory for Energy and Switching Electronics Systems, Department of Electrical and Computer Engineering, University of Illinois at Chicago, Chicago, IL 60607 USA (e-mail: mazumder@ece.uic.edu).

A. K. Rathore is with the Department of Electrical and Computer Engineering, National University of Singapore, Singapore, 117576 (e-mail: eleakr@nus.edu.sg).

Color versions of one or more of the figures in this paper are available online at <http://ieeexplore.ieee.org>.

Digital Object Identifier 10.1109/TIE.2010.2098375

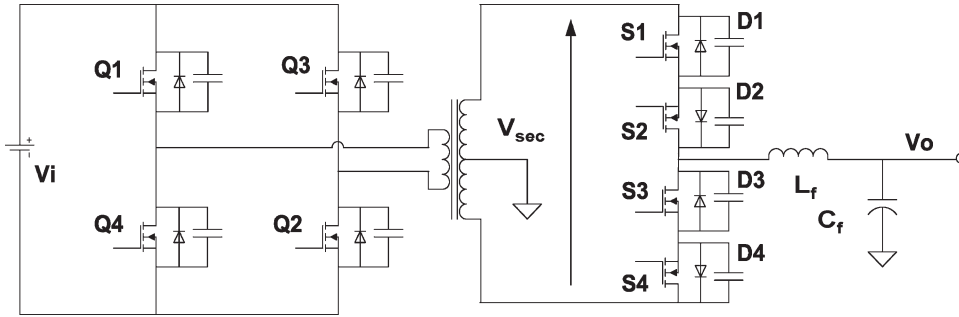


Fig. 1. CHFL inverter comprising a dc/ac and an ac/ac converter on the primary and secondary sides of the HF transformer.

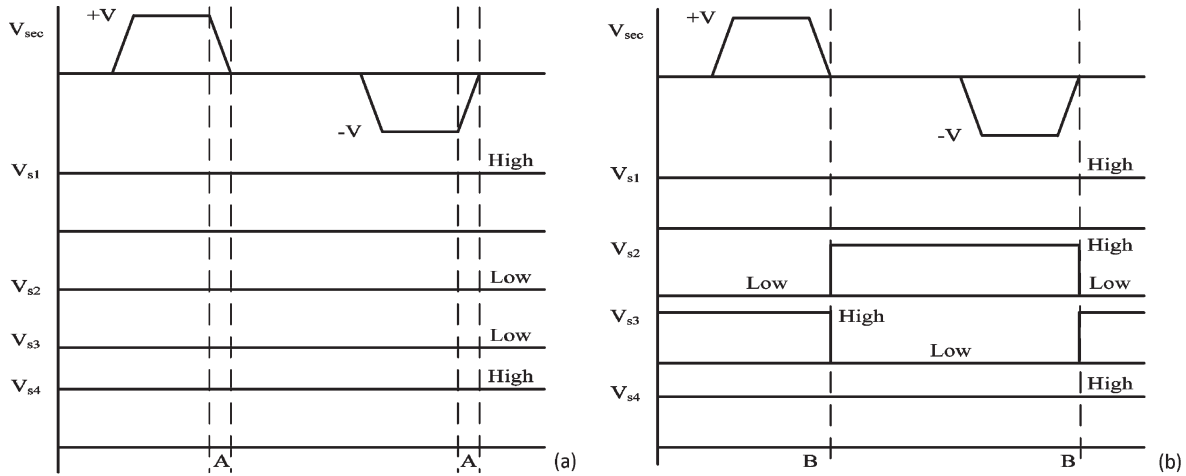


Fig. 2. Gating signals of the ac/ac converter for the “conventional scheme” when the polarities of the output voltage and output current are (a) the same and (b) opposite. The illustration in (a) is for positive output voltage and positive output current. The switching states are complementary if the output voltage and current are both negative. The illustration in (b) is for positive output voltage and negative output current. If the output voltage is negative and the output current is positive, the switching states will be complementary. The symbols L and H represent low and high switching states while  $+V$  and  $-V$  represent the minimum and maximum voltages of  $V_{sec}$ , which can be different from  $V_i$ .

this letter. The dc/ac converter produces an HF bipolar voltage ( $V_{sec}$ ) across the transformer using sinusoidal pulsewidth modulation. Bipolar voltage is required per switching cycle to ensure transformer flux balance.

For the conventional scheme and as illustrated in Fig. 2, the ac/ac converter has two operating scenarios: one with the polarities of the output voltage and output current being the same and the other with the polarities of the output voltage and output current being opposite. This is explained in detail in [20]. For the first scenario, the ac/ac converter switches operate at line frequency with the antiparallel diodes switching at HF (e.g., in the interval marked “A” in Fig. 2(a) in which the diodes turn off). For the second scenario, the half-bridge ac/ac-converter switches operate at HF [e.g., in the interval marked “B” in Fig. 2(b)] yielding higher switching loss.

For the ZVS scheme, the operating modes (for positive inverter output current and voltage,  $V_{sec} \geq 0$ , and  $V_{sec} \leq 0$ ) of the ac/ac converter are shown in Fig. 4, along with the switching sequences, which are shown in Fig. 3. The primary-side dc/ac converter dynamics is not illustrated. However, the voltage across the transformer secondary ( $V_{sec} = 0$  or  $V_{sec} > 0$ ) demonstrates that the primary-side dc/ac converter is operating in either the zero state or the active state. It is also noted that, even though the output of the dc/ac converter is bipolar, the

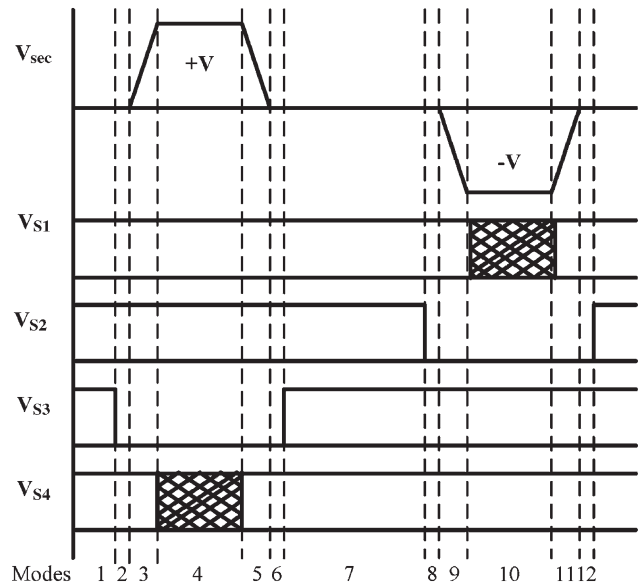


Fig. 3. Gating signals of the ac/ac converter for the “ZVS scheme” when the bipolar transformer secondary voltage is positive/negative.

principle of operation of the ZVS scheme does not change for negative primary-side voltage output. The operating modes are discussed below.

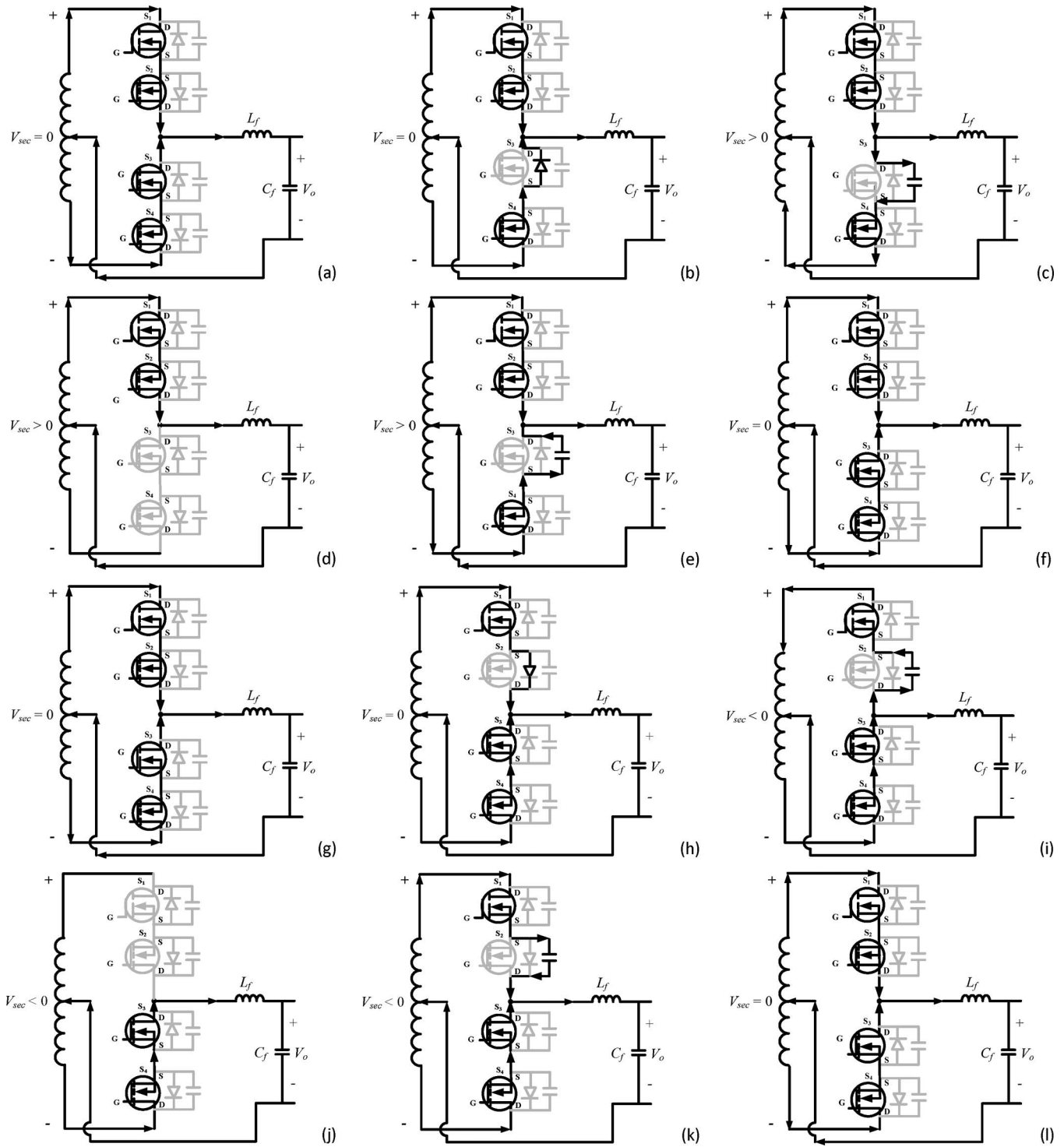


Fig. 4. Operating modes of the ac/ac converter for positive inverter output current and voltage using the dc/ac-converter-assisted ZVS scheme. (a)–(f)  $V_{sec} \geq 0$ . (g)–(l)  $V_{sec} \leq 0$ .

**Mode 1:** In this mode,  $V_{sec} = 0$ . All of the ac/ac-converter switches are turned on. As such, the output current is shared equally between the two arms of the half-bridge ac/ac converter. Note that the current sharing between the two arms results in lower conduction loss.

**Mode 2:** This is a zero-state interval during which  $V_{sec} = 0$ . At the beginning of Mode 2, the switch  $S_3$  is turned off under

ZVS condition. Half of the output current that was flowing through the lower arm now begins to transfer to the upper arm. Eventually, the switches  $S_1$  and  $S_2$  carry the output current.

**Mode 3:** This mode initiates when  $V_{sec}$  rises from zero voltage to the dc-bus level and ends with switch  $S_3$  blocking  $V_{sec}$ .

**Mode 4:** In this mode, switches  $S_1$  and  $S_2$  support the output current. Because switch  $S_3$  blocks  $V_{sec}$ , switch  $S_4$  can remain on, or it can be turned off under zero-current condition.

**Mode 5:** This mode initiates when the primary-side dc/ac converter attains a zero state, and as such,  $V_{sec}$  approaches zero voltage. The output current is primarily supported by switches  $S_1$  and  $S_2$  while the output capacitance of switch  $S_3$  discharges, and eventually, it is clamped by the antiparallel diode of  $S_3$ .

**Mode 6:** Similar to Mode 1, this is a zero-state interval. This mode ends when switch  $S_3$  turns on under ZVS condition. Subsequently, the output current is shared between the two arms of the ac/ac converter. At the end of this mode, a half switching cycle is achieved.

The other six modes (**Modes 7–12**) corresponding to positive output current and output voltage and  $V_{sec} \leq 0$  can be explained following the explanations for Modes 1–6 and are illustrated in Fig. 4.

### III. RESULTS

The efficacy of the ZVS scheme is ascertained using open-loop-control experiments on the CHFL inverter topology (shown in Fig. 1). The results of the ZVS scheme are also compared with the conventional scheme for the ac/ac converter. The dc/ac converter operates at 20 kHz which transforms to a 40-kHz PWM frequency at the output of the secondary-side ac/ac converter due to frequency doubling. The rated power of the inverter is 1 kW while the input voltage is set at 36 V. For the dc/ac converter, OptiMOS power MOSFETs (IPP08CN10N G) from Infineon are used, which have with following key specifications: voltage and current ratings of 100 V and 95 A, respectively, gate charge of 100 nC, and ON-state resistance of 8.2 mΩ. For the ac/ac converter, Q-class HiPerFET power MOSFETs (IXFX21N100Q) from IXYS are used. The key specifications of this device are as follows: voltage and current ratings of 1000 V and 21 A, respectively; gate-to-source and gate-to-drain stored charges of 27 and 18 nC, respectively; and ON-state resistance of 0.5 Ω. A nanocrystalline core (STX 1060M1) is used for the center-tapped HF transformer with the number of primary and secondary turns being 12 and 104 (i.e., 2 × 52), respectively. The values of the output filter inductance ( $L_f$ ) and capacitance ( $C_f$ ) are set to be 2.4 mH and 0.5 μF, respectively.

Fig. 5 shows the comparison of the inverter efficiencies obtained using the ZVS and conventional schemes. The inverter efficiency using the ZVS scheme shows an improvement of over 2% at the rated power and over 3% at around 20% of the rated power. Fig. 6(a) and (b) shows the overlapping gate-to-source and drain-to-source voltages for the conventional and ZVS schemes, illustrating a softer discharge mechanism for the ZVS scheme. Fig. 7 shows the impact of the enhanced efficiency using the ZVS scheme on the output voltage of the inverter. The results of the open-loop inverter clearly show a higher output-voltage yield for the ZVS scheme as compared to that of the conventional scheme due to the enhanced efficiency obtained using the former. Finally, Fig. 8 compares the THD

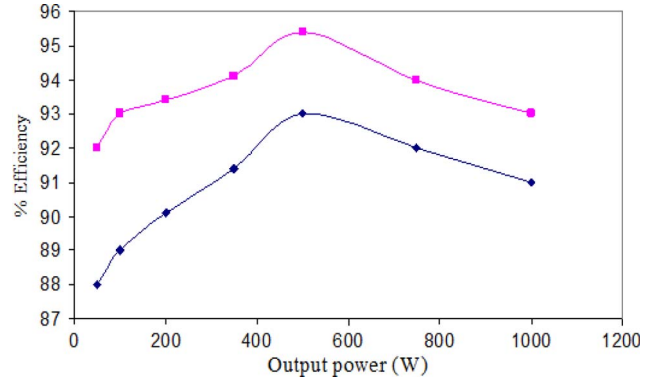
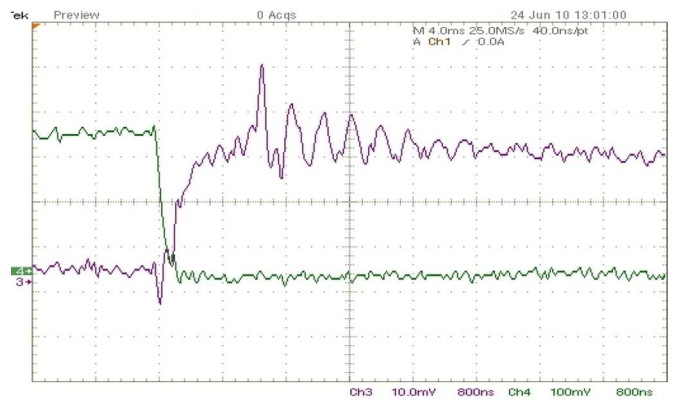
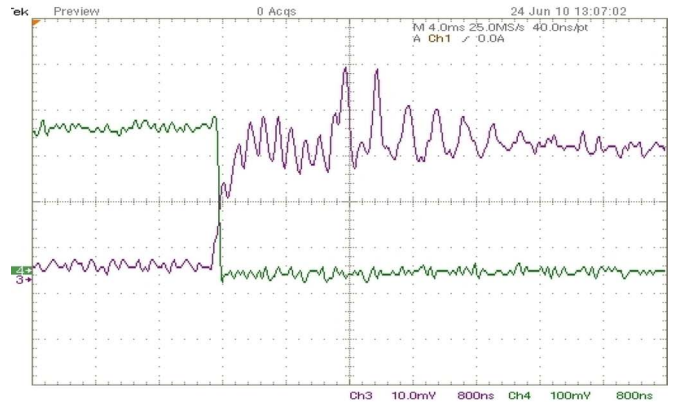


Fig. 5. Experimental comparison of the efficiencies of the (top trace) ZVS and (bottom trace) conventional schemes.



(a)



(b)

Fig. 6. MOSFET (falling trace) drain-to-source voltage and (rising trace) gate-to-source voltage for the ZVS and conventional schemes.

of the inverter output voltage using the ZVS and conventional schemes. The conventional scheme results in a small kink near the zero crossing. Hence, as the output power reduces and the switching effect becomes more dominant, the slight difference shows up as a small difference in the THD. However, at higher power, when the peak current is higher, the difference is negligible.

### IV. SUMMARY AND CONCLUSION

A new ZVS scheme for the ac/ac converter of a CHFL inverter has been outlined in this letter. By mitigating the device

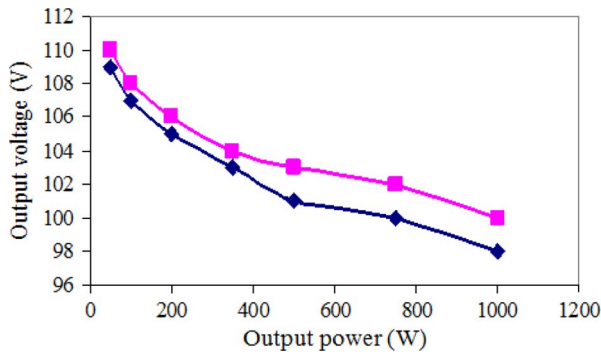


Fig. 7. Experimental output-voltage yield of the open-loop inverter with varying load demands for the (top trace) ZVS and (bottom trace) conventional schemes.

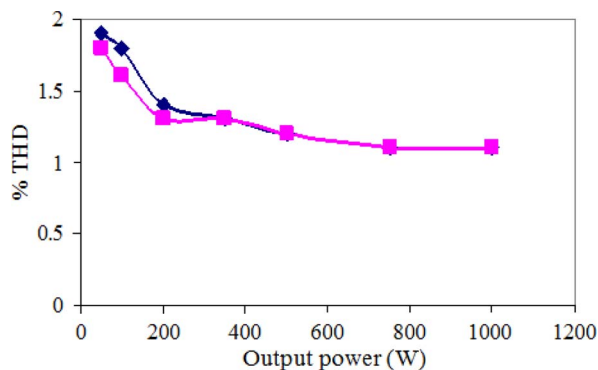


Fig. 8. Experimental THD of the inverter output voltage using the (bottom trace) ZVS and (top trace) conventional schemes.

switching loss, the ZVS scheme enables one to potentially choose power MOSFETs with lower ON-state resistance at the price of slightly higher output capacitance. Unlike the schemes outlined in [17]–[20], where a diode and an active device (e.g., MOSFET or IGBT) conduct during the transition and the ON-states, in the ZVS scheme, the diode only plays a small role during the transition. As such, the reverse recovery of the diode during the transition is reduced. These loss-mitigating mechanisms yield an improvement in the inverter (i.e., dc/ac converter followed by the ac/ac converter) efficiency of over 2% at the rated power and over 3% at around 20% of the rated power using the ZVS scheme. Aside from demonstrating the inverter efficiency using the ZVS scheme, we have also demonstrated the output-voltage yield and THD. They clearly show that a higher voltage and slightly better THD are yielded using the ZVS scheme due to higher efficiency and soft switching transition.

#### ACKNOWLEDGMENT

Any opinions, findings, conclusions, or recommendations expressed herein are those of the authors and do not necessarily reflect the views of the National Science Foundation. The novel soft-switching scheme outlined in this letter is covered by S. K. Mazumder, “A novel zero-voltage-switching scheme for photovoltaic/fuel-cell-based high-frequency-ac-link inverter,” USPTO Patent Application DC067, filed by the University of Illinois at Chicago, in 2009.

#### REFERENCES

- [1] M. Castilla, L. G. de Vicuña, J. Matas, J. Miret, and J. C. Vasquez, “A comparative study of sliding-mode control schemes for quantum series resonant inverters,” *IEEE Trans. Ind. Electron.*, vol. 56, no. 9, pp. 3487–3495, Sep. 2009.
- [2] B. D. Min, J. P. Lee, J. H. Kim, T. J. Kim, D. W. Yoo, and E. H. Song, “A new topology with high efficiency throughout all load range for photovoltaic PCS,” *IEEE Trans. Ind. Electron.*, vol. 56, no. 11, pp. 4427–4435, Nov. 2009.
- [3] S. Inoue and H. Akagi, “A bidirectional dc/dc converter for an energy storage system with galvanic isolation,” *IEEE Trans. Power Electron.*, vol. 22, no. 6, pp. 2299–2306, Nov. 2007.
- [4] H. Fujimoto, K. Kuroki, T. Kagotani, and H. Kidoguchi, “Photovoltaic inverter with a novel cycloconverter for interconnection to a utility line,” in *Conf. Rec. IEEE IAS Annu. Meeting*, 1995, pp. 2461–2467.
- [5] K. Wang, F. C. Lee, and W. Dong, “A new soft-switched quasi-single-stage (QSS) bi-directional inverter/charger,” in *Conf. Rec. IEEE IAS Annu. Meeting*, 1999, pp. 2031–2038.
- [6] E. Koutroulis, J. Chatzakis, K. Kalaitzakis, and N. C. Voulgaris, “Bidirectional, sinusoidal, high-frequency inverter design,” *Proc. Inst. Elect. Eng.—Elect. Power Appl.*, vol. 148, no. 4, pp. 315–321, Jul. 2001.
- [7] H. Cha and P. N. Enjeti, “A new soft switching direct converter for residential fuel cell power system,” in *Conf. Rec. IEEE IAS Annu. Meeting*, 2004, pp. 1172–1177.
- [8] L. S. Toh, Z. Salam, and M. Z. Ramli, “High-frequency transformer-link inverter with regenerative snubber,” in *Proc. IEEE Power Electron. Drive Syst. Conf.*, 2006, pp. 642–647.
- [9] R. Huang and S. K. Mazumder, “A novel soft-switching scheme for an isolated dc/dc converter with pulsating dc output for a three-phase high-frequency-link PWM converter,” *IEEE Trans. Power Electron.*, vol. 24, no. 10, pp. 2276–2288, Oct. 2009.
- [10] P. M. Espelage and B. K. Bose, “High-frequency link power conversion,” *IEEE Trans. Ind. Appl.*, vol. IA-13, no. 5, pp. 387–394, Sep. 1977.
- [11] S. Manias, P. D. Ziogas, and G. Olivier, “Bilateral dc to ac converter employing a high frequency link,” in *Conf. Rec. IEEE IAS Annu. Meeting*, 1985, pp. 1156–1162.
- [12] Z. Zansky, “Phase-modulated ac supply exhibits high efficiency,” *Electron Device Newsletter*, vol. 30, no. 22, pp. 177–180, Oct. 1985.
- [13] T. Kawabata, K. Honjo, N. Sashida, K. Sanada, and M. Koyama, “High frequency link dc/ac converter with PWM cycloconverter,” in *Conf. Rec. IEEE IAS Annu. Meeting*, 1990, pp. 1119–1124.
- [14] I. Yamato, N. Tokunaga, Y. Matsuda, Y. Suzuki, and H. Amaro, “High frequency link dc–ac converter for UPS with a new voltage clamper,” in *Proc. IEEE Power Electron. Spec. Conf.*, 1990, pp. 749–756.
- [15] I. Yamato and N. Tokunaga, “Power loss reduction techniques for three phase high frequency link dc–ac converter,” in *Proc. IEEE Power Electron. Spec. Conf.*, 1993, pp. 663–668.
- [16] M. Matsui, M. Nagai, M. Mochizuki, and A. Nabae, “High-frequency link dc/ac converter with suppressed voltage clamp circuits—naturally commutated phase angle control with self turn-off devices,” *IEEE Trans. Ind. Appl.*, vol. 32, no. 2, pp. 293–300, Mar./Apr. 1996.
- [17] K. Tazume, T. Aoki, and T. Yamashita, “Novel method for controlling a high-frequency link inverter using cycloconverter techniques,” in *Proc. IEEE Power Electron. Spec. Conf.*, 1998, pp. 497–502.
- [18] S. Deng, H. Mao, J. Mazumdar, I. Batarseh, and K. Islam, “A new control scheme for high-frequency link inverter design,” in *Proc. IEEE Appl. Power Electron. Conf.*, 2003, pp. 512–517.
- [19] J. Rocabert, M. Dumenjo, J. Bordonau, and J. A. B. Jimenez, “A regenerative active clamp circuit for dc/ac converters with high-frequency isolation in photovoltaic systems,” in *Proc. IEEE Power Electron. Spec. Conf.*, 2004, pp. 2082–2088.
- [20] R. Garcia-Gil, J. M. Espi, E. J. Dede, and E. E. Sanchis-Kilders, “A bidirectional and isolated three-phase rectifier with soft-switching operation,” *IEEE Trans. Ind. Electron.*, vol. 52, no. 3, pp. 765–773, Jun. 2005.
- [21] S. K. Mazumder, R. K. Burra, and K. Acharya, “A ripple-mitigating and energy-efficient fuel cell power-conditioning system,” *IEEE Trans. Power Electron.*, vol. 22, no. 4, pp. 1437–1452, Jul. 2007.
- [22] S. K. Mazumder, R. Burra, R. Huang, M. Tahir, K. Acharya, G. Garcia, S. Pro, O. Rodrigues, and E. Duheric, “A high-efficiency universal grid-connected fuel-cell inverter for residential application,” *IEEE Trans. Ind. Electron.*, vol. 57, no. 10, pp. 3431–3447, Oct. 2010.
- [23] D. De and V. Ramanarayanan, “A dc to three phase ac high frequency link converter with compensation for non-linear distortion,” *IEEE Trans. Ind. Electron.*, vol. 57, no. 11, pp. 3669–3677, Nov. 2010.



**Sudip K. Mazumder** (SM'03) received the M.S. degree in electrical power engineering from the Rensselaer Polytechnic Institute, Troy, NY, in 1993, and the Ph.D. degree in electrical and computer engineering from the Virginia Polytechnic Institute and State University, Blacksburg, in 2001.

He has over 15 years of professional experience and has held R&D and design positions in leading industrial organizations. He is currently the Director of the Laboratory for Energy and Switching Electronics Systems, Department of Electrical and Computer Engineering, University of Illinois at Chicago, Chicago, where he is also an Associate Professor. He has published over 100 refereed and invited journal and conference papers and is also the Editor of the book *Wireless Network Based Control* (Springer). He is a reviewer for multiple international journals and conferences. He was the Editor in Chief of the *Advances in Power Electronics Journal* between 2006–2009. His current research interests include interactive power electronics/power networks, renewable and alternate energy systems, photonically triggered and wide-bandgap power semiconductor devices, and applied technologies.

Dr. Mazumder has been an Associate Editor of the IEEE TRANSACTIONS ON POWER ELECTRONICS since 2009, of the IEEE TRANSACTIONS ON INDUSTRIAL ELECTRONICS since 2003, and of the IEEE TRANSACTIONS ON AEROSPACE AND ELECTRONIC SYSTEMS since 2008. He was an Associate Editor of the IEEE POWER ELECTRONICS LETTERS until 2005. He is the Chair of the Student/Industry Coordination Activities of the IEEE Energy Conversion Congress and Exposition for 2009 and 2010. Since 2009, he has also been the Vice Chair of the Technical Subcommittee on Distributed Generation and Renewable Energy. Between 2009–2010, he was also the Cochair of the IEEE Power Electronics Society (PELS) Committee on Sustainable Energy Systems. He has been invited by the IEEE and the American Society of Mechanical Engineers, as well as multiple industries, federal agencies, national laboratories, and universities, for several keynote, plenary, and invited lectures and presentations. He was the recipient of the prestigious 2008 and 2006 Faculty Research Awards from the University of Illinois for excellent scholarly work and outstanding research performance. He was also the recipient of the National Science Foundation CAREER Award and the Office of Naval Research Young Investigator Award in 2003 and 2005, respectively, and the recipient of the Prize Paper Award from the IEEE TRANSACTIONS ON POWER ELECTRONICS and the IEEE PELS in 2002. He was also the corecipient of the 2007 IEEE Outstanding Student Paper Award at the IEEE International Conference on Advanced Information Networking and Applications with Prof. M. Tahir. He was also the recipient of the 2005 IEEE Future Energy Challenge Energy Award.



**Akshay K. Rathore** (S'03) was born in Rajasthan, India. He received the B.E. degree in electrical engineering from the Maharana Pratap University of Agriculture and Technology, Udaipur, India, in 2001, the M.Tech. degree in electrical machines and drives from the Institute of Technology, Banaras Hindu University, Varanasi, India, in 2003, and the Ph.D. degree in power electronics from the University of Victoria, Victoria, BC, Canada, in 2008.

He was a Lecturer with the College of Technology and Engineering, Udaipur, and the Mody Institute of Technology and Science, Lakshamangarh, India, from February 2003 to August 2004. He was a Sessional Lecturer with the Department of Electrical and Computer Engineering, University of Victoria, from May to December 2007. He was a Research Fellow with the Electrical Machines and Drives Laboratory, University of Wuppertal, Wuppertal, Germany, from September 2008 to September 2009. He was a Postdoctoral Researcher Associate for one year with the University of Illinois at Chicago, Chicago, between 2009 and 2010. His research interests include soft-switching converters, high-frequency power conversion for distribution generation and renewable energy sources, modulation techniques, linear induction motors, and control of motor drives.

Dr. Rathore is a Reviewer of IEEE TRANSACTIONS, The Institution of Engineering and Technology, and Elsevier journals. He was listed in *Marquis Who's Who in Science and Engineering* in 2006, *Who's Who in the World*, and *Who's Who in America* in 2008.